

Nonlinear Corrections to the Momentum Sum Rule

G.R.Boroun*

Department of Physics, Razi University, Kermanshah 67149, Iran

(Dated: December 8, 2023)

The importance of the nonlinear corrections on the momentum sum rule is investigated on the initial scale Q_0^2 . Nonlinear corrections are found to play an indispensable role in the singlet and gluon momentum sum rule in the high-order approximations in the parameterization groups for nucleons and light nuclei at low x in future colliders. In this way, we obtain a significantly different low x behavior of the singlet and gluon momentum sum rule at the hotspot point.

1. Introduction

Sum rules are integrals over structure functions or parton distributions, which are extremely useful in calculating the lowest-mass hadronic bound states or determining effective coupling constants. The starting point for QCD sum rules is the operator-product expansion (OPE), which was formulated firstly by M.A.Shifmann, A.I.Vainshtein and V.I.Zakharov in Ref.[1]. The QCD sum rules are a phenomenological procedure for evaluating the matrix elements of the operators that occur, and OPE gives a general form for the quantities of interest [2]. The matrix elements of the operators in the OPE for the forward virtual Compton amplitude $\gamma^*p \rightarrow \gamma^*p$ correspond with the Mellin moments of the structure functions [3]. Sometimes the origin of a sum rule is more fundamental than the quantum parton model (QPM). We might call a sum rule an exact QCD sum rule if its result found within the context of the parton model is not altered by any radiative or non-perturbative correction [4,5]. The first one is the Adler [6] sum rule, where it is for the charged current structure functions and follows from the current conservation. The Bjorken [7] and Gross-Llewellyn [8] sum rules get a QCD correction, where the parton model results are modified by radiative corrections. The Gottfried [9] sum rule requires the assumption of an SU(2) symmetric sea and is affected by non-perturbative physics.

The momentum sum rule (MSR) has been seen as a convenient constraint on the definition of the parton distribution functions (PDFs) rather than a basic QCD sum rule when going beyond leading order QCD. The sum of the fraction of the proton's momentum carried by quarks must be less than unity and the remaining momentum is carried by the gluons. Botje in Ref.[10] was shown that integral over the PDFs for quarks and gluons at the initial scale Q_0^2 gives $\int_0^1 dx x \sum_q (q(x) + \bar{q}(x)) = 0.594 \pm 0.018$ and $\int_0^1 dx x g(x) = 0.394 \pm 0.018$ where $\sum_q (q + \bar{q})$ is the

flavor-singlet contribution and g is the gluon distribution. In fact the gluons carry the very large missing fraction of the proton momentum. The MSR from the second Mellin moment reads

$$\int_0^1 dx x \left[\sum_q (q(x, Q_0^2) + \bar{q}(x, Q_0^2)) + g(x, Q_0^2) \right] = 1, \quad (1)$$

and modified by the following form

$$\int_0^1 dx x \left[u_v(x, Q_0^2) + d_v(x, Q_0^2) + S(x, Q_0^2) + g(x, Q_0^2) \right] = 1, \quad (2)$$

where the light quark sea contribution is defined as $S \equiv 2(\bar{u} + \bar{d}) + s + \bar{s}$.

In order to make a precise determination of parton distribution sets (such as CTEQ, nCTEQ, MSTW, GRV, GJR and NNPDF Collaborations), one has to use a large set of data which together cover a large range of x and Q^2 and put stringent constraints on the various parton types within the proton. Usually the following parameterizations for gluon and sea quark distributions are used by the above groups at the initial scale Q_0^2 . As an example we have

$$x f_i(x, Q_0^2) = A_i x^{\delta_i} (1-x)^{\eta_i} (1 + \epsilon_i \sqrt{x} + \gamma_i x). \quad (3)$$

The values of the parameters obtained from a global QCD fit and also the normalization parameters are fixed by the MSR and valence quark counting rules¹. Differences in the results of different groups are made from many subjective choices in the selection of data sets and kinematic boundaries, together with the choice of the strong coupling constant and the correction for non-perturbative and target mass and nuclear effects of data from fixed target experiments [4].

In this paper we consider the nonlinear corrections (NLCs) to the momentum sum rule and show differences in the MSR due to PDF sets in LO, NLO and NNLO at α_s for nucleons and nuclei. In the next section,

*Electronic address: boroun@razi.ac.ir

¹ $\int_0^1 dx x u_v(x, Q_0^2) = 2$ and $\int_0^1 dx x d_v(x, Q_0^2) = 1$.

the theoretical formalism is presented, including the nonlinear corrections at the initial scale.

2. Nonlinear Corrections

The nonlinear corrections (or gluon recombination effects) are not negligible in the low x , low Q^2 region and it is known that this behavior reduces the growth of the gluon distribution. These nonlinear effects were defined by Gribov-Levin-Ryskin [11] and Mueller-Qiu [12] (GLR-MQ). The main difference of this equation from the Linear evolution equation is the presence of the quantity, G^2 which is interpreted as the two-gluon distribution per unit area of hadron. The dominant source for the nonlinear corrections at low x is the conversion of the two gluon ladders merged into a gluon or a quark-antiquark pair, as the evolution of the parton distributions is directly related to the gluon-gluon fusion terms in the GLR-MQ evolution equations [13,14]. Indeed, this leads to saturation of the gluon density at low Q^2 with decreasing x , when $W \lesssim \alpha_s$ where $W = \frac{n_g \hat{\sigma}}{\pi R^2} \sim \frac{\alpha_s(Q^2)}{\pi R^2 Q^2} xg(x, Q^2)$. Here, n_g is the number of gluons, $\hat{\sigma}$ is the gluon-gluon cross section and πR^2 is the transverse area of a hadron where R is the characteristic radius of the gluon distribution in the hadronic target, which determines the strength of the nonlinear corrections and it comes from the integration over the transverse components of k (k is the transverse momenta of gluons), $\frac{1}{R^2} \sim \int dk_T^2 [F(-k_T^2)]^2$. When gluon ladders are coupled to the proton radius, then the value of R is given by $R = 5 \text{ GeV}^{-1}$. Indeed, the form factor F is characterized by the proton radius. The value $R = 2 \text{ GeV}^{-1}$ signifies the gluons concentrated on the hotspots [15-17]. Although a more precise nonlinear evolution equation was developed by Balitsky-Kovchegov [18,19] based on the evolution of BFKL, but to study the possible importance of shadowing we base our starting gluon and singlet distributions $g(x, Q_0^2)$ and $S(x, Q_0^2)$ on the solutions of the GLR-MQ evolution equation based on Refs.[15,16].

On the basis of the shadowing effects, the nonlinear corrections to the MSR read

$$\int_0^1 dx x \left[u_v(x, Q_0^2) + d_v(x, Q_0^2) + S^{\text{NLC}}(x, Q_0^2) + g^{\text{NLC}}(x, Q_0^2) \right] = 1, \quad (4)$$

where

$$xg^{\text{NLC}}(x, Q_0^2) = xg(x, Q_0^2)\xi^{\text{NLC}}(x, x_0, Q_0^2), \quad (5)$$

and

$$\xi^{\text{NLC}}(x, x_0, Q_0^2) = \left\{ 1 + \theta(x_0 - x) \left[xg(x, Q_0^2) - xg(x_0, Q_0^2) \right] / xg_{\text{sat}}(x, Q_0^2) \right\}^{-1}, \quad (6)$$

with

$$xg_{\text{sat}}(x, Q^2) = \frac{16R^2Q^2}{27\pi\alpha_s(Q^2)}, \quad (7)$$

where g_{sat} is the value of the gluon which would saturate the unitarity limit in the leading shadowing approximation. The parameter x_0 is introduced to be $x_0 \simeq 10^{-2}$ so that the nonlinear corrections are negligible for $x \geq x_0$. The nonlinear corrections to the gluon distribution are reflected in the sea-quark distributions where the sea-quark starting distribution in the region $x < x_0$ is proportioned to the nonlinear correction to the gluon by the following form [15,16]

$$xS^{\text{NLC}}(x, Q_0^2) = xS(x, Q_0^2)\xi^{\text{NLC}}(x, x_0, Q_0^2). \quad (8)$$

Therefore the NLCs to the MSR is defined by

$$\int_0^1 dx x \left[u_v(x, Q_0^2) + d_v(x, Q_0^2) + \xi^{\text{NLC}}(x, x_0, Q_0^2) \left\{ S(x, Q_0^2) + g(x, Q_0^2) \right\} \right] = 1. \quad (9)$$

It is useful to consider the linear and nonlinear corrections to the singlet and gluon distribution functions in which the kernel P_{s+g} reads

$$P_{s+g}^{\text{NLC}}(x, Q_0^2) = \xi^{\text{NLC}}(x, x_0, Q_0^2) (xS(x, Q_0^2) + xg(x, Q_0^2)), \quad (10)$$

where the momentum sum rule for single and gluon distributions is defined by

$$I_{s+g}^{\text{NLC}} = \int_0^1 P_{s+g}^{\text{NLC}}(x, Q_0^2) dx. \quad (11)$$

The NLCs to the MSR in a nucleus are modified owing to by the nuclear modification factor $w_i(x, A, Z)$, as

$$\int_0^1 dx x \left[u_v^A(x, Q_0^2) + d_v^A(x, Q_0^2) + \xi_A^{\text{NLC}}(x, x_0, Q_0^2) \left\{ S^A(x, Q_0^2) + g^A(x, Q_0^2) \right\} \right] = 1, \quad (12)$$

where the initial nuclear parton distributions at a fixed Q_0^2 are defined by the following form

$$f_i^A(x, Q_0^2) = w_i(x, A, Z) f_i(x, Q_0^2), \quad (13)$$

where the modification function, based on the QCD analysis, in a cubic type is

$$w_i(x, A, Z) = 1 + \left(1 - \frac{1}{A^\alpha} \right) \frac{a_i(A, Z) + H_i(x)}{(1-x)^{\beta_i}}, \quad (14)$$

where $H_i(x) = b_i(A)x + c_i(A)x^2 + d_i(A)x^3$ is available in the literature [20-23]. The value of R^A for a nuclear target with the mass number A , in the nuclear gluon

saturation xg_{sat}^A , is defined by $R^A = A^{1/3}R$ [24]. The momentum sum rule for single and gluon distributions in nuclei modified by the following form

$$I_{sA+gA}^{\text{NLC}} = \int_0^1 P_{sA+gA}^{\text{NLC}}(x, Q_0^2) dx \quad (15)$$

where

$$P_{sA+gA}^{\text{NLC}}(x, Q_0^2) = \xi_A^{\text{NLC}}(x, x_0, Q_0^2)(xS^A(x, Q_0^2) + xg^A(x, Q_0^2)). \quad (16)$$

The results that are obtained in the above (i.e., Eqs.11 and 16) can be confirmed by simulating the events in eA collisions at the large hadron electron collider (LHeC) [25] and the Electron-Ion Collider (EIC) [26] energies in future.

3. Results and Conclusions

We begin by specifying the parametrization of the singlet and gluon distributions via the global parton analysis² of MSTW 2008 collaboration, where the optimal values of α_s and the input singlet and gluon parameters at $Q_0^2 = 1 \text{ GeV}^2$ in the LO up to NNLO approximations are determined and summarized in Ref.[27]. The values $\alpha_s(M_Z^2)$ at the LO, NLO and NNLO approximations are the values of 0.13939, 0.12018 and 0.11707 respectively. The new singlet and gluon distributions from the CT18 collaboration³ are used at the initial scale $Q_0^2 = 1.69 \text{ GeV}^2$ in the NNLO approximation where in Ref.[28] $\alpha_s(M_Z^2) = 0.1164$. Nuclear singlet and gluon distribution functions⁴ in a general mass variable flavor number scheme have been called from Ref.[29], where the CT18 PDFs are used as baseline proton PDFs and the strong coupling constant is taken as $\alpha_s(M_Z^2) = 0.118$. In Ref.[30], the singlet and gluon distributions from JR09 collaboration⁵ in the NNLO approximation at the initial scale $Q_0^2 = 2 \text{ GeV}^2$ with $\alpha_s(M_Z^2) = 0.1158$. The

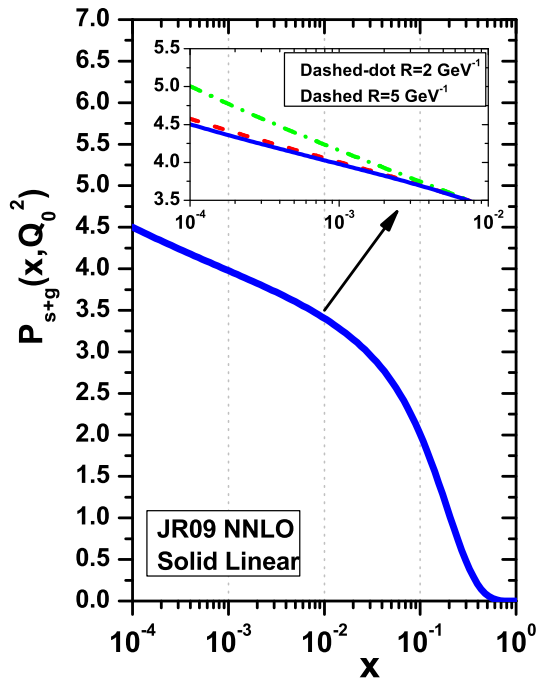


FIG. 1: $P_{s+g}(x, Q_0^2)$ as a function of x on the initial scale $Q_0^2 = 2 \text{ GeV}^2$ for the JR09 parameterization model [30] in the NNLO approximation. The inset: the nonlinear corrections compared with the linear (solid curve) at $R = 5 \text{ GeV}^{-1}$ (dashed curve) and $R = 2 \text{ GeV}^{-1}$ (dashed-dot curve) for $x \leq 10^{-2}$.

nPDFs⁶ at the NNLO approximation are obtained from Refs.[21,22] where all parton distributions are obtained from JR09 [30] and CT18 [28] set of the free proton PDFs, respectively.

Figures 1 and 2 show the kernel $P_{s+g}(x, Q_0^2)$ (i.e., Eq.(10)) for the linear ($\xi^{\text{NLC}}(x, x_0, Q_0^2) = 1$) correction at the input scale $Q_0^2 = 2 \text{ GeV}^2$ and 1.69 GeV^2 in a wide range of x for the JR09 [30] and CT18 [28] parameterization models in the NNLO approximation, respectively. The nonlinear ($\xi^{\text{NLC}}(x, x_0, Q_0^2) \neq 1$) corrections are compared with the linear in the region $x \leq 10^{-2}$ for both $R = 2 \text{ GeV}^{-1}$ (dashed-dot curves) and $R = 5 \text{ GeV}^{-1}$ (dashed curves) in Figs.1 and 2. We observe that the kernel $P_{s+g}(x, Q_0^2)$ is violated [31] at low x if we consider the nonlinear corrections at the hotspot. These violations

² The parton distributions are determined in the NLO and NNLO approximations from the global analysis of hard-scattering data within the standard framework of leading-twist fixed-order collinear factorization in the $\overline{\text{MS}}$ scheme [27].

³ The new PDFs from the CTEQ-TEA collaboration, obtained using a wide variety of high-precision Large Hadron Collider (LHC) data, in addition to the combined HERA I+II deep-inelastic scattering data set in the NNLO approximation [28].

⁴ The nuclear deep-inelastic scattering data analyzed in Ref.[29] are complemented by the available charged current neutrino DIS data with nuclear targets and data from Drell-Yan cross section measurements for several nuclear targets in the NLO and NNLO approximations.

⁵ The deep inelastic scattering and Drell-Yan dimuon production data in the NNLO approximation are available [30].

⁶ The nuclear parton distribution functions (nPDFs) are obtained from neutral current charged-lepton deeply inelastic scattering data and Drell-Yan (DY) cross-section ratios $\sigma_{DY}^A/\sigma_{DY}^{A'}$ for several nuclear targets in the NNLO approximation [21].

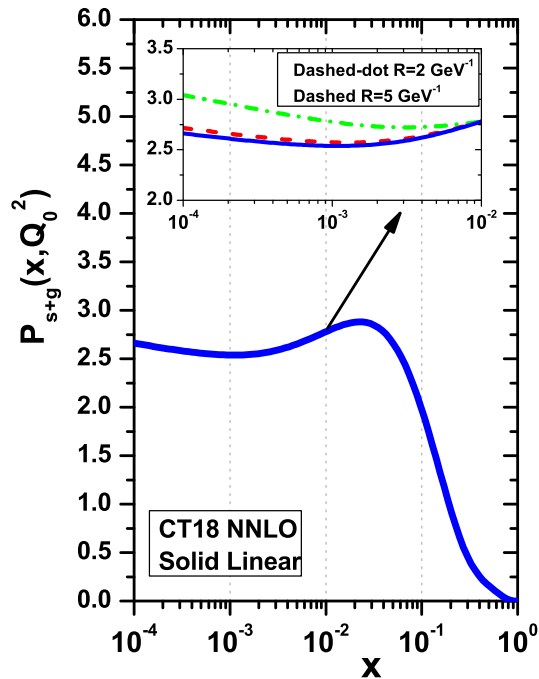


FIG. 2: $P_{s+g}(x, Q_0^2)$ as a function of x on the initial scale $Q_0^2 = 1.69 \text{ GeV}^2$ for the CT18 parameterization model [28] in the NNLO approximation. The inset: the nonlinear corrections compared with the linear (solid curve) at $R = 5 \text{ GeV}^{-1}$ (dashed curve) and $R = 2 \text{ GeV}^{-1}$ (dashed-dot curve) for $x \leq 10^{-2}$.

are visible at low x for the JR09 and CT18 parameterization models. As we see from Figs.1 and 2, accounting for nonlinear corrections gives a noticeably larger linear singlet+gluon at low x at the hotspot point.

In Tables I and II, the singlet and gluon contributions to the MSR (i.e., I_{s+g}) by the nonlinear corrections at $R = 5 \text{ GeV}^{-1}$ and $R = 2 \text{ GeV}^{-1}$ are compared. We compare the linear of I_{s+g} with the nonlinear corrections for the MSTW parameterization model [27] in the LO, NLO and NNLO approximations on the initial scale $Q_0^2 = 1 \text{ GeV}^2$. In Table II, we compared the linear and nonlinear corrections to the singlet and gluon contributions of the MSR on the initial scale $Q_0^2 = 2 \text{ GeV}^2$ for the JR09 parameterization model [30] and on the initial scale $Q_0^2 = 1.69 \text{ GeV}^2$ for the CT18 parameterization model [28] in the NNLO approximation respectively, at $R = 5 \text{ GeV}^{-1}$ and $R = 2 \text{ GeV}^{-1}$. The differences between the linear and nonlinear corrections for the singlet and gluon contributions in the momentum sum rule are defined by the following form

$$\Delta = I_{s+g}^{\text{Linear}} - I_{s+g}^{\text{Nonlinear}}(R). \quad (17)$$

We observe in Tables I and II that the nonlinear corrections to the MSR increase the singlet and gluon contributions⁷ in comparison with the linear at the initial scales. Indeed, the momentum carried by the singlet and gluon distributions increases when we consider the nonlinear corrections to the distribution functions at the initial scales. By having these corrections at

TABLE I: I_{s+g} on the initial scale $Q_0^2 = 1 \text{ GeV}^2$ for the MSTW parameterization model [27] in the LO, NLO and NNLO approximations. The nonlinear corrections obtained at $R = 5 \text{ GeV}^{-1}$ and $R = 2 \text{ GeV}^{-1}$ respectively. The differences between the linear and nonlinear corrections for the singlet and gluon contributions in the momentum sum rule are determined.

I_{s+g}	LO	NLO	NNLO
Linear	0.5219817	0.5150395	0.5137795
Nonlinear($R = 5 \text{ GeV}^{-1}$)	0.5213362	0.5151779	0.5138630
Nonlinear($R = 2 \text{ GeV}^{-1}$)	0.5222538	0.5193943	0.5095848
$\Delta(R = 5 \text{ GeV}^{-1})$	0.0006455	-0.0001385	-0.000834
$\Delta(R = 2 \text{ GeV}^{-1})$	-0.0002721	-0.0043549	0.0041947

TABLE II: I_{s+g} on the initial scale $Q_0^2 = 2 \text{ GeV}^2$ for the JR09 parameterization model [30] and on the initial scale $Q_0^2 = 1.69 \text{ GeV}^2$ for the CT18 parameterization model [28] in the NNLO approximation respectively. The nonlinear corrections obtained at $R = 5 \text{ GeV}^{-1}$ and $R = 2 \text{ GeV}^{-1}$ respectively. The differences between the linear and nonlinear corrections for the singlet and gluon contributions in the momentum sum rule are determined.

I_{s+g}	JR09	CT18
Linear	0.5451307	0.5404662
Nonlinear($R = 5 \text{ GeV}^{-1}$)	0.5452354	0.5406253
Nonlinear($R = 2 \text{ GeV}^{-1}$)	0.5458140	0.5404662
$\Delta(R = 5 \text{ GeV}^{-1})$	-0.0001047	-0.0001591
$\Delta(R = 2 \text{ GeV}^{-1})$	-0.0006833	-0.0010523

low x , it will be possible to redefine the MSR for the parameters on the singlet and gluon distributions for all sets of parametrizations at the starting scale Q_0^2 in future colliders. This provides a mechanism regulating the respective amounts of nonlinear corrections at low x [32].

A main observable consequence is extracting nonlinear corrections to the momentum sum rule for nuclei⁸. Figures 3-5 show the kernel $P_{sA+gA}(x, Q_0^2)$ (i.e., Eq.(16)) for the linear ($\xi_A^{\text{NLC}}(x, x_0, Q_0^2) = 1$) correction at the input scale $Q_0^2 = 2 \text{ GeV}^2$ and 1.69 GeV^2 in a wide range of x for the JR09 [30] and CT18 [28] parameterization

⁷ For all parameterization groups considered.

⁸ An interesting novel correction to the MSR for nuclear structure functions is addressed by the authors in Ref.[32].

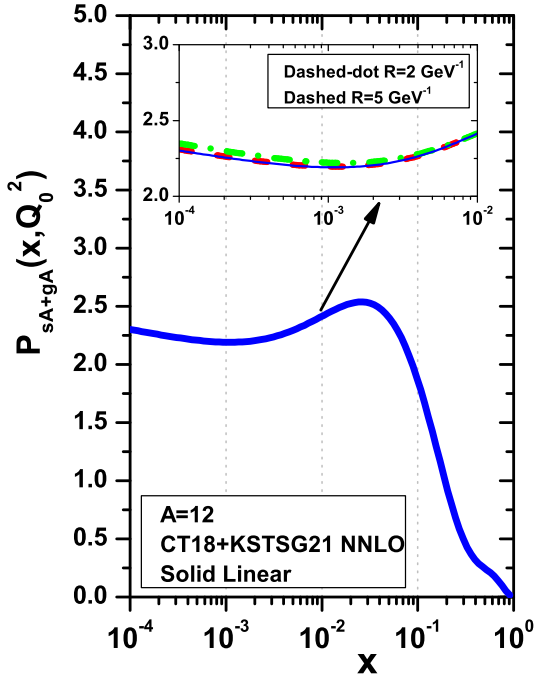


FIG. 3: $P_{sA+gA}(x, Q_0^2)$ as a function of x on the initial scale $Q_0^2 = 1.69 \text{ GeV}^2$ for the CT18 [28] and KSTSG21 [29] parameterization models in the NNLO approximation of the nucleus of C-12 ($A=12, Z=6$). The inset: the nonlinear corrections compared with the linear (solid curve) at $R = 5 \text{ GeV}^{-1}$ (dashed curve) and $R = 2 \text{ GeV}^{-1}$ (dashed-dot curve) for $x \leq 10^{-2}$.

models in the NNLO approximation, respectively, where the nuclear modifications are provided by a weight function⁹ $w_i(x, A, Z)$ by the KT16 [21] and KSTSG21 [29] respectively. The nonlinear ($\xi_A^{\text{NLC}}(x, x_0, Q_0^2) \neq 1$) corrections are compared with the linear in the region $x \leq 10^{-2}$ for both $R = 2 \text{ GeV}^{-1}$ (dashed-dot curves) and $R = 5 \text{ GeV}^{-1}$ (dashed curves) for the light and heavy nuclei in Figs.3-5. In these figures (i.e., Figs.3-5) we observe that the violation of the nonlinear kernel $P_{sA+gA}^{\text{NLC}}(x, Q_0^2)$ from the linear behavior is observable for the light nuclei at low x at the hotspot point $R = 2 \text{ GeV}^{-1}$. These violations of the linear behavior are visible at low x for light nuclei, although they are small (see Fig.3), and they are invisible for heavy nuclei independent of the parametrization groups (see Figs.4 and 5).

⁹ The nuclear PDFs are related to the PDFs in a free proton by multiplying a weight function $w_i(x, A, Z)$ at the input scale.

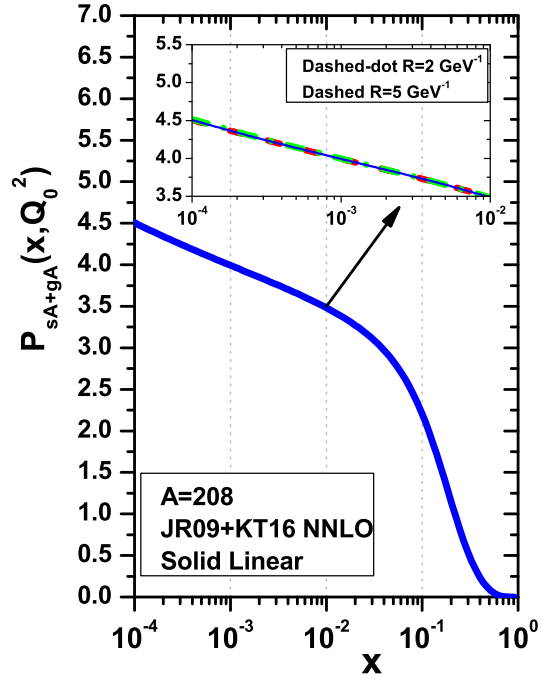


FIG. 4: $P_{sA+gA}(x, Q_0^2)$ as a function of x on the initial scale $Q_0^2 = 2 \text{ GeV}^2$ for the JR09 [30] and KT16 [21] parameterization models in the NNLO approximation of the nucleus of Pb-208 ($A=208, Z=82$). The inset: the nonlinear corrections compared with the linear (solid curve) at $R = 5 \text{ GeV}^{-1}$ (dashed curve) and $R = 2 \text{ GeV}^{-1}$ (dashed-dot curve) for $x \leq 10^{-2}$.

The deviations of the MSR, according to the nonlinear corrections, for light and heavy nuclei are shown in Table III. In Table III, we compared the linear and nonlinear corrections to the I_{sA+gA} for the heavy nucleus of Pb-208 on the initial scale $Q_0^2 = 2 \text{ GeV}^2$ where the nPDFs are obtained from the JR09 [30] set of the free proton PDFs by weight functions $w_i, i = s, g$ are obtained from the KT16 [21] set of the nPDFs. Also, the linear and nonlinear corrections to the I_{sA+gA} for the heavy nucleus of Pb-208 and the light nucleus of C-12 on the initial scale $Q_0^2 = 1.69 \text{ GeV}^2$ are illustrated in Table III, where the nPDFs are obtained from the CT18 [28] set of the free proton PDFs by weight functions $w_i, i = s, g$ are defined from the KSTSG21 [29] set of the nPDFs. The nonlinear corrections and their differences are obtained at $R^A = A^{1/3} \times 5 \text{ GeV}^{-1}$ and $R^A = A^{1/3} \times 2 \text{ GeV}^{-1}$ respectively. These differences in I_{sA+gA} can be considered in the light nuclei at the hotspot point, but they are very small in the heavy nuclei. Additionally, we furnish several predictions of the ratio $R = \frac{I_{sA+gA}}{A I_{s+g}}$ in the JR09 and CT18 sets for the

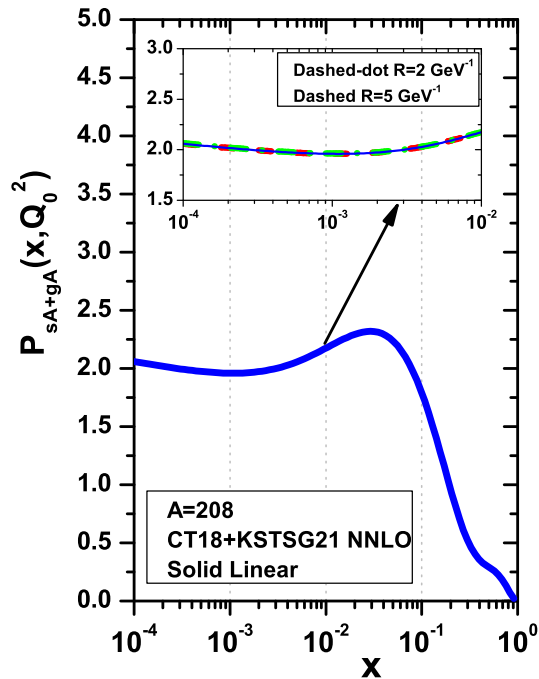


FIG. 5: $P_{sA+gA}(x, Q_0^2)$ as a function of x on the initial scale $Q_0^2 = 1.69 \text{ GeV}^2$ for the CT18 [28] and KSTSG21 [29] parameterization models in the NNLO approximation of the nucleus of Pb-208 ($A=208, Z=82$). The inset: the nonlinear corrections compared with the linear (solid curve) at $R = 5 \text{ GeV}^{-1}$ (dashed curve) and $R = 2 \text{ GeV}^{-1}$ (dashed-dot curve) for $x \leq 10^{-2}$.

nuclei C-12 and Pb-208 in Table IV, to be probed at upcoming collider experiments such as EIC, as they are expected to improve the precision of MSR at low- x .

In summary, we have investigated the effects of nonlinear corrections to the momentum sum rule at the initial scale Q_0^2 . Using the shadowing effects at low x and the known parton distribution functions, we are able to add nonlinear corrections to the momentum sum rule for the nucleons and nuclei. Interestingly, these effects increase the description of the singlet and gluon contributions to the momentum sum rule at the beginning of low Q^2 evolution. The main effect is to increase the singlet and gluon contributions to the momentum sum rule for the proton and the light nuclei at very low x at the hotspot point, which can be helpful for the upcoming LHeC and EICs.

TABLE III: I_{sA+gA} on the initial scale $Q_0^2 = 2 \text{ GeV}^2$ for the JR09 and KT16 [21] parameterization models [30] and on the initial scale $Q_0^2 = 1.69 \text{ GeV}^2$ for the CT18 and KSTSG21 [29] parameterization models [28] in the NNLO approximation for the nuclei of C-12 ($A=12, Z=6$) and Pb-208 ($A=208, Z=82$) respectively. The nonlinear corrections obtained at $R = 5 \text{ GeV}^{-1}$ and $R = 2 \text{ GeV}^{-1}$ respectively. The differences ($\Delta^A = I_{sA+gA}^{\text{Linear}} - I_{sA+gA}^{\text{Nonlinear}}(R)$) between the linear and nonlinear corrections for the singlet and gluon contributions in the momentum sum rule for the light and heavy nuclei are determined.

I_{sA+gA}	JR09	CT18	CT18
Nuclei	A=208	A=12	A=208
Linear	0.5939293	0.5562324	0.5619174
Nonlinear($R = 5 \text{ GeV}^{-1}$)	0.5939323	0.5562545	0.5619200
Nonlinear($R = 2 \text{ GeV}^{-1}$)	0.5939482	0.5563717	0.5619338
$\Delta^A(R = 5 \text{ GeV}^{-1})$	-0.30×10^{-5}	-0.0000221	-0.26×10^{-5}
$\Delta^A(R = 2 \text{ GeV}^{-1})$	-0.0000189	-0.0001394	-0.0000165

TABLE IV: Ratio $R = \frac{I_{sA+gA}}{AI_{s+g}}$ for the JR09 and CT18 sets in the NNLO approximation for the nuclei of C-12 and Pb-208 at $R = 5 \text{ GeV}^{-1}$ and $R = 2 \text{ GeV}^{-1}$.

$R = \frac{I_{sA+gA}}{AI_{s+g}} \times 10^{-2}$	JR09	CT18	CT18
Nuclei	A=208	A=12	A=208
Linear	0.52380	8.57640	0.49985
Nonlinear($R = 5 \text{ GeV}^{-1}$)	0.52370	8.57430	0.49971
Nonlinear($R = 2 \text{ GeV}^{-1}$)	0.52317	8.57860	0.49987

ACKNOWLEDGMENTS

I am grateful to Razi University for the financial support of this project.

REFERENCES

- M.A.Shifmann, A.I.Vainshtein and V.I.Zakharov, Nucl.Phys.B **147**, 385 (1979).
- W.Greiner and A.Schafer, Quantum Chromodynamics, Springer 1994.
- K.Golec-Biernat and Anna M.Stasto, Phys.Rev.D**107**, 054020 (2023); S.J.Brodsky, I.Schmidt and S.Liuti, arXiv[hep-ph]:1908.06317.
- G.Dissertori, I.Knowles and M.Schmelling, Quantum Chromodynamics, High Energy Experiments and Theory, Oxford University Press (2003).
- R.G.Roberts, The Structure of the proton, Deep Inelastic Scattering, Cambridge University Press (1990).
- S.L.Adler, Phys.Rev. **143**, 1144 (1966).
- J.D.Bjorken, Phys.Rev. **163**, 1767 (1967).
- D.J.Gross and C.H.Llewellyn Smith, Nucl.Phys.B**14**, 337 (1969).

9. K.Gottfried, Phys.Rev.Lett.**18**, 1154 (1967).
10. M.Botje, Eur.Phys.J.C **14**, 285 (2000).
11. L. V. Gribov, E. M. Levin and M. G. Ryskin, Phys. Rept. **100**, 1 (1983).
12. A. H. Mueller and J. w. Qiu, Nucl. Phys. B **268**, 427 (1986).
13. M.R.Pelicer et al., Eur.Phys.J.C **79**, 9 (2019).
14. V.A.Abramovsky, V.N.Gribov, O.V.Kancheli, Yad. Fiz. **18**, 595 (1973); Sov.J.Nucl.Phys. **18**, 308 (1974).
15. J.Kwiecinski et al., Phys.Rev.D **42**, 3645 (1990).
16. J.Collins and J.Kwiecinski, Nucl.Phys.B **335**, 89 (1990).
17. M.Lalung, P.Phukan and J.K.Sarma, Nucl.Phys.A **984**, 29 (2019); G.R.Boroun, arXiv:2305.04243; G.R.Boroun and B.Rezaei, Eur.Phys.J.C **81**, 851 (2021).
18. I.Balitsky, Nucl.Phys.B **463**, 99 (1996).
19. Y.V.Kovchegov, Phys.Rev.D **60**, 034008 (1999).
20. M.Hirai, S.Kumano and M.Miyama, Phys. Rev. D **64**, 034003 (2001).
21. H.Khanpour and S.Atashbar Tehrani, Phys.Rev.D **93**, 014026 (2016).
22. H.Khanpour et al., Phys.Rev.D **104**, 034010 (2021); S.Atashbar Tehrani, Phys.Rev.C **86**, 064301 (2012).
23. M. Hirai, S. Kumano and T.-H. Nagai, Phys. Rev. C **70**, 044905 (2004).
24. J.Rausch, V.Guzey and M.Klasen, Phys.Rev.D **107**, 054003 (2023); G.R.Boroun, B.Rezaie and F.Abdi, arXiv:2305.01893; G.R.Boroun and B.Rezaei, arXiv:2303.07654; Phys.Rev.C **107**, 025209 (2023); F. Muhammadi and B.Rezaei, Phys.Rev.C **106**, 025203(2022).
25. LHeC Collaboration, FCC-he Study Group, P. Agostini, et al., J. Phys. G, Nucl. Part. Phys. **48**, 110501 (2021).
26. R.Abdul Khalek et al., Nucl. Phys.A **1026**, 122447 (2022).
27. A.D.Martin, W.J.Stirling, R.S.Thorne and G.Watt, Eur.Phys.J.C **63**, 189 (2009).
28. Tie-Jiun Hou et al., Phys.Rev.D **103**, 014013 (2021).
29. H.Khanpour et al., Phys.Rev.D **104**, 034010 (2021).
30. P.Jimenez-Delgado and E.Reya, Phys.Rev.D **79**, 074023 (2009).
31. G.C.Nayak, arXiv [hep-ph]:1804.02712; 1806.01220.
32. S.J.Brodsky, V.E.Lyubovitskij and I.Schmidt, Phys.Lett.B **824**, 136812 (2022).